Journal of Pharmaceutical Sciences 114 (2025) 103894

Contents lists available at ScienceDirect

Journal of Pharmaceutical Sciences

journal homepage: www.elsevier.com/locate/xphs

Pharmaceutics, Drug Delivery and Pharmaceutical Technology

Impact of drug-polymer complexation and media properties on the release performance of amorphous solid dispersions containing a weakly basic drug and hydroxypropyl methylcellulose acetate succinate

Amanpreet Kaur [a], Dmitry Zemlyanov [b], Lynne S. Taylor [a,*]

[a] Department of Industrial and Molecular Pharmaceutics, College of Pharmacy, Purdue University, West Lafayette, IN 47907, USA
[b] Birck Nanotechnology Center, Purdue University, West Lafayette, IN 47907, USA

ARTICLE INFO

Keywords:
HPMCAS
Bedaquiline
Ion-pair complex
Biorelevant media
Recrystallization

ABSTRACT

Herein, the release performance of amorphous solid dispersions (ASDs) of a weakly basic drug, bedaquiline (BDQ), and a weakly acidic polymer, hydroxypropyl methylcellulose acetate succinate (HPMCAS) was investigated in different media. In conjunction, the complexation tendency between BDQ and HPMCAS was also probed. Amorphous solid dispersions (ASDs) of BDQ were prepared at different drug loadings with LF and MF grades of HPMCAS using solvent evaporation. Drug-polymer complexation was investigated in buffers varying in pH from 5.8 to 10.5 and in biorelevant media. For these experiments, polymer concentration was quantified using colorimetry or high-performance liquid chromatography (HPLC) and evaporative light scattering detection (ELSD). The insoluble drug-polymer complex formed in some media was analyzed using attenuated total reflectance-Fourier transform infrared (ATR-FTIR) spectroscopy. Drug release from ASD powders was evaluated as a function of pH (1.6, 3.0, 5.0, 6.5) as well as in fasted and fed state simulated intestinal fluids. HPMCAS showed a high degree of insoluble complex formation (~90 %) with BDQ at pH 6.0 and the extent of complexation decreased with increasing pH, or when biorelevant media was used. At pH 6.5, ASDs showed a low extent of release in buffer. Release of drug from the ASDs was considerably enhanced in biorelevant media. BDQ remained amorphous in the presence of HPMCAS for extended time periods, hence crystallization was not considered a failure mechanism. Instead, the low release extent observed in pH 6.5 buffer was attributed to the formation of an insoluble BDQ:polymer ionic complex in the ASD particle. Ionic complexation was confirmed using X-ray photoelectron spectroscopy. However, it appears that solubilizing species present in the biorelevant media disrupted the drug-polymer complexation leading to improved release. These studies highlight the convoluted nature of drug release from ASDs with enteric polymers and the need to consider the impact of the release testing conditions. Release as a function of media conditions, is in turn expected to be highly variable from drug to drug depending on the nature of the drug-polymer interactions.

Introduction

Amorphous solid dispersion (ASD) is a well-utilized formulation strategy for improving solubility and dissolution rate of drugs with poor aqueous solubility. Upon release under non-sink conditions, an ASD ideally forms a supersaturated solution, improving the drug membrane transport rate and bioavailability.[1] In ASDs, the lipophilic drug is molecularly dispersed in a hydrophilic polymer matrix. The polymer kinetically stabilizes the drug, preventing desupersaturation as well as recrystallization from the solid matrix.[2,3] Polymers achieve stabilization in the solid state by several mechanisms including reducing molecular mobility, formation of drug-polymer intermolecular interactions and via a reduction in the chemical potential of the drug.[4] A review of marketed products shows that poly(1-vinylpyrrolidone-co-vinyl acetate) (PVPVA), hydroxypropyl methylcellulose acetate succinate (HPMCAS), polyvinylpyrrolidone (PVP), polymethacrylates, hydroxypropyl methylcellulose (HPMC), and hydroxypropyl methylcellulose phthalate (HPMCP), are examples of polymers used for ASD formulations.[5,6]

Development of an appropriate release testing method is critical to assess different ASD formulations, confirming that extensive release occurs, and that supersaturation is maintained for biologically relevant time periods. Drug release mechanisms from ASDs are complex and are

* Corresponding author.
E-mail addresses: chahal3@purdue.edu (A. Kaur), dzemlian@purdue.edu (D. Zemlyanov), lstaylor@purdue.edu (L.S. Taylor).

https://doi.org/10.1016/j.xphs.2025.103894
Received 18 February 2025; Received in revised form 20 June 2025; Accepted 27 June 2025
Available online 6 July 2025
0022-3549/© 2025 The Authors. Published by Elsevier Inc. on behalf of American Pharmacists Association. This is an open access article under the CC BY-NC-ND license (http://creativecommons.org/licenses/by-nc-nd/4.0/).

not fully understood. Release is governed by the physicochemical properties of both drug and polymer with important factors including pKa, ionization extent, precipitation and crystallization tendencies.[3,7,8] Important media properties that can influence release include buffer species, buffer capacity, pH, and the presence or absence of additional solubilizing species such as micelles. Polymers such as PVPVA and HPMC are non-ionic and dissolve in aqueous media independent of the pH. However, enteric polymers such as HPMCP and HPMCAS are pH-sensitive and only dissolve when sufficiently ionized, typically at pH >5.0-5.5.[9,10] Several studies have demonstrated that the dissolution of HPMCAS-containing ASDs is complicated as a result of factors including the ionization requirement of the polymer, surface pH effects, and insoluble drug-polymer complex formation with lipophilic cationic drugs arising from electrostatic interactions between oppositely charged groups.[11–14] Drug release from HPMCAS-containing ASDs appears to be controlled by polymer dissolution, in particular at lower drug loadings. Importantly, because of polymer ionization and the subsequent release of protons, the pH of the unstirred water layer adjacent to the dissolving ASD surface can be lower than that of the bulk pH.[15] A lowered surface pH can, in turn, retard the dissolution of HPMCAS. Moreover, the presence of drug molecularly dispersed in the ASD reduces water sorption during hydration, impeding polymer dissolution.[14] Drug-polymer ionic interactions have also been proposed as a mechanism by which polymer release is impeded, specifically for enteric polymers. It was suggested that ASDs of lumefantrine (weak base, pKa of 8.7) and HPMCAS (weak acid, pKa of ~5) ASDs exhibited poor release due to the formation of drug-polymer ionic interactions at pH 6.8, impeding hydration of polymer carboxylate groups, which in turn reduced polymer dissolution.[16] Subsequent investigations supported the conjecture that lipophilic cationic drugs reduce HPMCAS solubility due to the formation of a hydrophobic electrostatic complex at the gel-layer interface, as well as in bulk solution, resulting in poor drug release, even at drug loadings as low as 5 %.[11] However, HPMCAS is of great interest as an ASD polymer due to its excellent crystallization inhibition properties for many drugs.[9]

The goal of the current study was to investigate insoluble drug-polymer complex formation between a weakly basic drug, bedaquiline (BDQ), and HPMCAS in different media. The hypothesis was that drug-polymer complexation would be reduced at higher pH conditions where BDQ was less ionized, and by the presence of the solubilizing components present in simulated intestinal media. BDQ belongs to the diarylquinoline class of anti-tubercular drugs. It was discovered by Janssen in 2002 and approved by the U.S. Food and Drug Administration (FDA) in 2012 as a part of a combination therapy for pulmonary multidrug-resistant tuberculosis in adult and pediatric patients.[17] BDQ (molecular weight of 555.50 g/mol) is a weakly basic drug with a pKa of 8.5 (determined experimentally, supplementary information) and a log P of 7.13.[18,19] It is practically insoluble in water (<1 μg/mL) and belongs to Class II of the Biopharmaceutics Classification System (BCS).[18,20] It is recommended that BDQ is administered with food to improve absorption.[18] It is a good candidate for formulation as ASD, because it has both solubility and dissolution rate limited absorption. In the current study, we explored correlations between ASD release performance and the extent of insoluble complex formation. The hypothesis to be tested was that for media conditions where a high extent of insoluble complex formation was observed, release from the ASD would be low. Conversely, a higher extent of release was expected to occur in media where little insoluble complex formation was noted. We prepared ASDs of BDQ with HPMCAS (LF and MF grades) using solvent evaporation. Release profiles of ASDs were determined at pH 5.8, 6.5 and in biorelevant media. To study complexation between BDQ and HPMCAS, stock solutions containing different molar ratios of drug to the COOH groups of HPMCAS were added to buffers with different pH values, as well as simulated intestinal fluids, considering the ionization extent of both drug and polymer. After centrifugation, the supernatant was analyzed for polymer concentration, while the pellet was analyzed using attenuated total reflectance-Fourier transform infrared (ATR-FTIR) spectroscopy. Nucleation induction times of BDQ were also evaluated in select media to eliminate crystallization as a failure mechanism.

Materials

Bedaquiline (BDQ) was supplied by J-Star Research, Inc (Cranbury, NJ). The chemical structure of BDQ is provided in Figure S1. Hydroxypropylmethylcellulose acetate succinate (HPMCAS) LF and MF grades were procured from Shin-Etsu Chemical Co., Ltd (Tokyo, Japan). Buffer components, namely sodium phosphate dibasic/ monobasic monohydrate, sodium acetate, sodium hydroxide, sodium chloride, acetic acid, phosphoric acid, trifluoroacetic acid, formic acid and hydrochloric acid were purchased from Fisher Scientific (Pittsburgh, PA). Acetonitrile, acetone and dichloromethane were also procured from Fisher Scientific. Fasted state simulated intestinal fluid (FaSSIF)-V1, fed state simulated intestinal fluid (FeSSIF)-V1/V2 buffers and powders were purchased from Biorelevant (London, UK). Deionized water, generated in-house, was used for preparing buffers for dissolution and HPLC analysis.

Methods

Amorphous solid dispersions (ASDs) of BDQ

ASDs were prepared by solvent evaporation using a Hei-VAP Core rotary evaporator (Heidolph Instruments, Schwabach, Germany) equipped with an EcoChyll S Chiller (Ecodyst, Apex, NC). BDQ and polymers were dissolved in a 1:1 v/v mixture of acetone and dichloromethane at a total solids content of 5 % w/v. ASDs were prepared at varying drug-polymer weight ratios of 5:95, 10:90, 20:80 and 30:70. Rotary evaporation was performed at 50 °C under vacuum over a 20 min period. ASDs were subjected to a vacuum for an additional 48 h to remove any residual solvent. ASDs were then milled using a 6775 Freezer/Mill (Cole-Parmer, Metuchen, NJ). The vial was pre-cooled in liquid N_2 for 2 min and subjected to cryomilling at 10 cps for 1 min for total of 4 cycles with a 1 min cool time for each cycle. The milled powder was passed through a mesh 60 (250 μm) and the undersize fraction was used for further characterization and analysis.

Modulated differential scanning colorimetry (mDSC)

DSC analysis of the ASDs was carried out using a DSC 2500 (TA Instruments, New Castle, DE) equipped with Refrigerated Cooling System (RCS 90). Samples (2–3 mg each) were weighed in a Tzero aluminum pan, sealed using a Tzero press and subjected to mDSC analysis at a modulation amplitude of ±0.500 °C every 60 s from 25 to 200 °C/min at 5 °C/min. Dry nitrogen was purged continuously during the analysis at 50 mL/min. The instrument was calibrated for temperature and enthalpy using indium.

Powder X-Ray diffraction (PXRD)

PXRD analysis was performed using a SmartLab diffractometer (Rigaku, Tokyo, Japan) in Bragg−Brentano mode with a Cu-kα radiation source and D/tex ultra detector, operated at 40 kV and 40 mV. Powder samples were filled into the cavity of the quartz holder and pressed level using a clean glass slide. PXRD patterns were collected in continuous mode within an angular range of 5 to 40° at a step size of 0.01°/s.

Thermodynamic solubility

Buffers (5 mL) were filled into 20 mL glass scintillation vials and kept in a 1 L jacketed beaker maintained at 37±0.5 °C. Excess crystalline BDQ powder was added to each vial and stirred using a magnetic stirrer at 500 rpm for 48–72 h until equilibrium concentrations were achieved.

Undissolved BDQ was separated from each buffer by ultracentrifugation at 35,000 rpm for 30 min at 37 °C using an Optima l-100 XP centrifuge (Beckman Coulter, Brea, CA). The supernatant (2 mL) was collected for quantification of BDQ concentration. A pH reading was taken for each solution prior to analysis.

BDQ concentration was determined using a 1260 Infinity II High-Pressure Liquid Chromatography (HPLC) system (Agilent Technologies, Santa Clara, CA). A reverse-phase BDS-Hypersil C_{18}, 150 × 4.6 mm, 5 µm column (Thermo Scientific, Swedesboro, NJ) was used with acetonitrile and water (containing 0.1 % trifluoroacetic acid) in a ratio of 70:30 v/v in isocratic mode at 1 mL/min. The injection volume was 10 µL and BDQ was detected at 210 nm using an ultraviolet (UV) detector. Linear calibration curves with an R^2 of 0.999 were prepared from 1 mg/mL stock solution of BDQ prepared in acetonitrile in the concentration range of 1 to 100 µg/mL. The LOD and LOQ values were determined to be 1 ± 0.5 µg/mL and 3.5 ± 0.2 µg/mL, respectively.

Amorphous solubility

Amorphous solubility of BDQ in different buffers was determined using the ultracentrifugation method.[21] A 20 mg/mL stock solution of BDQ was prepared in dimethyl sulfoxide (DMSO). Buffers (5 mL) were filled into 20 mL glass scintillation vials and maintained at 37±0.5 °C in a jacketed beaker. To each buffer, a 50–100 µL aliquot of DMSO stock was added under stirring at 300 rpm. Immediately after formation of a precipitate, the solution was transferred to a polypropylene tube followed by ultracentrifugation at 37,000 rpm for 30 min at 37 °C. The supernatant (1 mL) was transferred to a HPLC vial for quantification of BDQ concentration using the HPLC method given in section 3.4. The pH of each buffer solution was measured before analysis.

BDQ-HPMCAS LF/MF complexation

Complexation of BDQ and HPMCAS LF/MF was investigated in pH 5.8 buffer (blank FeSSIF-V2), FeSSIF-V2, pH 6.0 buffer, pH 6.5 buffer (blank FaSSIF-V1), FaSSIF-V1, and pH 7.0, 8.5 and 10.5 buffers. The detailed composition of each buffer is compiled in Table SI. For complexation experiments, 5 mL of buffer was added to a 20 mL glass scintillation vial stirred at 990 rpm using a multistage magnetic stirrer. Stock solutions consisting of BDQ and HPMCAS were prepared as per Table 1. THF was chosen for preparation of stock solutions because both BDQ and HPMCAS had appreciable solubility in THF. In each stock solution, the concentration of BDQ was varied, while that of HPMCAS was kept constant at 25 mg/mL, in order to change the molar ratio of BDQ to the number of moles of HPMCAS COOH groups. The number of millimoles of acid per gram of polymer was taken from previous studies conducted in our lab.[16,22]

A 100 µL aliquot of the stock solution (Table 1) was added to 5 mL of buffer solution. As a control, a polymer stock solution of HPMCAS LF or MF was also prepared without BDQ in THF, which gave a transparent solution after adding to buffer at a concentration of 0.5 mg/mL. Blank FeSSIF-V2 and blank FaSSIF-V1 did not shown any change in pH during the experiment. Buffers at pH 6.0, 7.0, 8.5 and 10.5 showed a pH decrease of 0.2 to 0.5 units due to polymer ionization and release of H^+ ions (Table SII). Following addition of the stock solution, solutions were stirred for 30 min, transferred to polypropylene tubes, and subjected to ultracentrifugation at 35,000 rpm, for 30 min at 25 °C. HPMCAS concentration in the supernatant were determined either using colorimetry or an HPLC system equipped with an evaporative light scattering detector (ELSD). For the colorimetry method, the supernatant was diluted appropriately using the corresponding buffer. To 400 µL of the diluted supernatant, 10 µL phenol (4 g in 1 mL of purified water) was added followed by vortexing for 30 s. Subsequently, 1 mL of concentrated H_2SO_4 was added, vortexed for 30 s and the samples were allowed to develop color for 1 h. Absorbance was measured at 490 nm using a Cary 300 Bio UV–Visible Spectrophotometer (Varian, Agilent Technologies, Santa Clara, CA). HPMCAS LF/MF calibration curves were prepared in each buffer over the concentration range of 1 to 50 µg/mL and were used for quantification of polymer concentrations in test and control samples. For calibration curves constructed in presence of different buffers, the LOD and LOQ values were in the range of 1.2 to 3.5 µg/mL and 3.5 to 5 µg/mL, respectively.

Polymer concentrations in FaSSIF-V1 and FeSSIF-V1/V2 media were determined using a 1260 Infinity II HPLC equipped with ELSD (Agilent Technologies, Santa Clara, CA). The mobile phase comprised of acetonitrile and water (both containing 0.1 % formic acid) run through a Shodex RSpak DS-413 column (Resonac, New York, NY) in gradient mode. The details of the gradient method are given in Table SIII. Liquid nitrogen was continuously flushed through the ELSD detector at 1.5 L/min. The nebulizer and evaporator temperatures were maintained at 80 °C and 85 °C, respectively. A polymer stock solution (1 mg/mL) was prepared in buffer at pH 6.5 and diluted with methanol to provide samples in the concentration range of 1 to 100 µg/mL which were used to build a calibration curve with R^2 of 0.997–0.999. The LOD and LOQ values for calibration curves for L/M grades of polymer in different buffers were in the range of 2.5 to 3.5 µg/mL and 4 to 5.5 µg/mL, respectively.

A decrease in polymer concentration in the supernatant indicated complexation with BDQ, where the insoluble drug-polymer complex sedimented upon ultracentrifugation. The polymer concentrations in each test sample supernatant (addition of both drug and polymer) were compared to the control sample (wherein only polymer was added) to calculate the percentage of polymer complexation with BDQ.

Attenuated total reflectance-fourier transform infrared spectroscopy (ATR-FTIR)

The insoluble residue obtained after ultracentrifugation in the complexation experiment was dried overnight under vacuum and analyzed using a Vertex 70 IR spectrophotometer (Bruker, Billerica, MA) and a Golden Gate ATR assembly (Specac, Orpington, Kent, UK). ATR-FTIR spectra were collected over the wavenumber range of 3700–650 cm^{-1} at a resolution of 4 cm^{-1} where 64 scans were co-added where spectra were converted to absorbance units.

Release testing

ASD powder dissolution was performed using a Hanson Vision

Table 1
BDQ-HPMCAS stock solution concentrations for the complexation experiment.

Molar ratio of BDQ: COOH groups of HPMCAS LF	Equivalent to loading in ASD (%) Drug: Polymer	Stock in THF (mg/mL)	Molar ratio of BDQ: COOH groups of HPMCAS MF	Equivalent to loading in ASD (%) Drug: polymer	Stock in THF (mg/mL)
R1- 0.0625:1	5.1:94.9	1.34:25	0.08:1	5.0:95.0	1.32:25
R2- 0.125:1	9.6:90.4	2.67:25	0.16:1	9.6:90.4	2.64:25
R3- 0.3:1	20.4:79.6	6.42:25	0.4:1	20.9:79.1	6.61:25
R4- 0.5:1	30.0:70.0	10.69:25	0.65:1	30.1:69.9	10.74:25
R5- 0.8:1	40.6:59.4	17.11:25	1:1	39.8:60.2	16.52:25
R6- 1.2:1	50.7:49.3	25.66:25	1.5:1	49.8:50.2	24.78:25

Classic 6 dissolution apparatus (Teledyne Labs, Essex, UK) equipped with a Pion Rainbow Dynamic Dissolution Monitor (East Sussex, UK). Initial release in buffers of pH 1.6, 3.0 and 5.0 was coupled with a pH switch after 1 h to 6.5 through addition of a predetermined amount of concentrated phosphate buffer (3–5 mL). The final volume of the dissolution medium was 50 mL. Single stage release in pH 6.5, FaSSIF-V1, FeSSIF-V1 and V2 was performed in 50 mL of media in 150 mL vessels. The media was maintained at 37±0.5 °C and stirred at 150 rpm using paddles. ASD powder, equivalent to a 5 mg dose of BDQ (100, 50, 25 and 16.66 mg, respectively, for 5, 10, 20 and 30 % drug loading ASDs) was added to each vessel, leading to a maximum theoretical concentration of 100 μg/mL. BDQ concentrations were recorded using a 2 mm in situ fiber optic dip probe with spectra collected at 1 min intervals for a total of 120 min. All experiments were performed in triplicate.

Nucleation induction time measurement

Nucleation induction time was measured by the scattering method using an SI Photonics CCD Array UV–Vis Spectrophotometer (Tucson, AZ).[23] The buffer of interest (5 mL) was filled into a 20 mL glass scintillation vial and maintained at 37±0.5 °C in a 50 mL jacketed beaker. A 0.5 cm SI Photonics fiber optic dip probe attached to the spectrophotometer was immersed in the buffer for automatic, real-time collection of UV–vis spectra in the range of 200 to 450 nm. Buffer was stirred at 300 rpm and a 50 μl aliquot of 20 mg/mL stock of BDQ (dissolved in DMSO) was added to the buffer to achieve a final concentration of 100 μg/mL. In each buffer, the induction time was measured in the absence and presence of a polymer (dissolved at a concentration of 400 μg/mL). Spectra (a total of 145) were collected at every 10 min over a time frame of 24 h. At the end of the experiment, each sample was visualized under cross polarizers using an E200 Nikon Eclipse light microscope (Melville, NY) and a 10 X objective. Additionally, droplet/particle size of each sample was measured by dynamic light scattering using a Nano-ZS Zetasizer Nanoseries (Malvern Panalytical, Worcestershire, UK).

X-ray photoelectron spectroscopy (XPS)

Various samples, including BDQ, its maleate salt, an amorphous solid dispersion (ASD) with 40 % drug load, and insoluble material from a complexation experiment, were analyzed by X-ray photoelectron spectroscopy (XPS). Wet samples were dried overnight under vacuum before analysis. XPS spectra were acquired using a Kratos Axis Ultra DLD spectrophotometer (Kratos Analytical Inc., Manchester, UK) with monochromatic Al Kα radiation (1486.6 eV) at constant pass energies of 20 eV for high-resolution spectra and 160 eV for survey spectra. A Kratos charge neutralizer was employed to mitigate surface charge on non-conductive powder samples during data acquisition, enhancing resolution. The instrument resolution at 20 eV pass energy was approximately 0.35 eV. Binding energy (BE) values were referenced to the Fermi level, with the BE scale calibrated using Au $4f_{7/2}$ at 84.0 eV and Cu $2p_{3/2}$ at 932.67 eV. Powders were mounted on a stainless-steel sample holder using double-sided copper tape. XPS data were analyzed using CasaXPS software, with charge correction applied by setting the C—C component of the C 1 s peak to 284.8 eV. Atomic concentrations in the near-surface region (~10 nm) were estimated after Shirley or Tougaard background subtraction. Curve fitting was conducted with Gaussian/Lorentzian peak shapes, using protonated and unprotonated N 1 s components from BDQ maleate to assess nitrogen ionization. C 1 s peaks were fitted using model peaks from pure BDQ and HPMCAS to determine surface drug and polymer concentrations. For each sample, 3–5 spots were analyzed.

Results

Solid-state characterization of BDQ ASDs

The results for solid-state characterization of ASDs using DSC and PXRD are compiled in Figure S2 and S3, respectively, in the supplementary file. All ASDs were X-ray amorphous and showed a single glass transition event.

Crystalline and amorphous solubility of BDQ in different media

Crystalline and amorphous solubility values of BDQ in different media of interest are given in Table 2. BDQ is a weakly basic drug with a pKa of 8.5, and therefore, showed maximum crystal solubility in pH 1.6 buffer. Both crystalline and amorphous solubilities dropped notably in buffers with higher pH. In biorelevant media, the crystalline solubility was substantially increased in the order of FeSSIF-V1>FeSSIF-V2>FaSSIF-V1, which was dictated by both the pH of the medium and the amount of solubilizing species, with the latter factor likely predominating. Amorphous solubilities could not be determined at low pH or in biorelevant media, but can be anticipated to be >20 fold higher than the crystalline solubility values.

BDQ-HPMCAS complexation

BDQ and HPMCAS have pKa values of 8.5 and 4.97 respectively. Ionization of BDQ and HPMCAS leads to formation of cationic and anionic species respectively, which can then form an insoluble complex due to ion-pair interactions. Figs. 1 and 2 show the percent polymer complexation at different molar ratios of BDQ to COOH groups of LF and MF, respectively. The complexation of BDQ and HPMCAS was investigated in media with different pH values to evaluate the impact of varying the extent of drug and polymer ionization. Complexation was only studied in media where the polymer was sufficiently ionized to be soluble in the absence of the drug. For example, blank FeSSIF-V1 was not used because at a pH of 5.0, HPMCAS has limited solubility (~250 and 110 μg/mL, for LF and MF, respectively).[13] In contrast, in pH 5.8 buffer, HPMCAS formed a clear solution and thus had a solubility greater than the target value of 0.5 mg/mL. Similar observations were made for higher pH buffers. Thus, HPMCAS alone is soluble at pH 5.8 and above.

For LF, the trend of polymer complexation extent as a function of initial pH was as follows 6.0 > 5.8 > 6.5 > 7.0 > 8.5 > 10.5. MF (Fig. 2) showed a similar trend. For both polymers, an increase in the molar ratio of BDQ led to an increase in polymer complexation with plateau values greater than 85–90 % complexation being reached at pH 5.8 and 6.0, whereby virtually no polymer remained soluble in the aqueous phase. With an increase in pH, polymer complexation reduced from >90 % at pH 6.0 to < 5 % at pH 10.5. Blank FaSSIF-V1 (pH 6.5) and blank FeSSIF-V2 (pH 5.8) had ~50 % and ~85 % polymer complexation respectively for BDQ:COOH molar ratios of 0.5:1, 0.8:1 and 1.2:1 (these ratios are equivalent to those found in ~30, 40 and 50 % drug loading ASDs, respectively). Complexation was notably reduced in FaSSIF-V1 and

Table 2
Solubility of BDQ in different media. The values have been represented as Mean ±SD ($N = 3$).

Media	Crystalline solubility (μg/mL)	Amorphous solubility (μg/mL)
Buffer pH 1.6	67.1 ± 0.1	-
Buffer pH 3.0	21.6 ± 0.3	-
Buffer pH 5.0	0.52±0.01	13.4 ± 0.5
Buffer pH 5.8*	<0.1	1.9 ± 0.4
Buffer pH 6.5**	Undetected	0.63±0.02
FaSSIF-V1	7.8 ± 0.3	-
FeSSIF-V1	628±11	-
FeSSIF-V2	258.8 ± 1.2	-

*Blank FeSSIF-V2 and **Blank FaSSIF-V1 without the micelles.

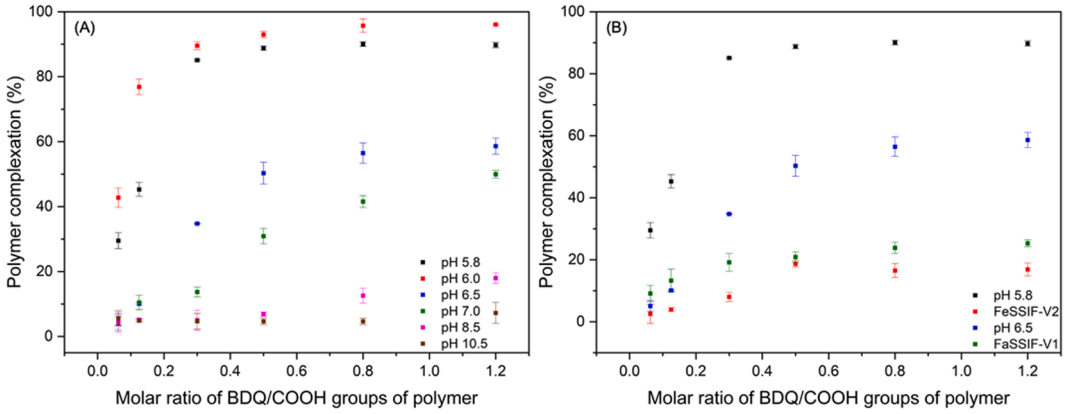


Fig. 1. Percent polymer complexation at different molar ratios of BDQ to COOH groups of HPMCAS LF in (A) initial pH 5.8, 6.0, 6.5, 7.0, 8.5, or 10.5 buffer and (B) in initial pH 5.8 or 6.5 buffer, FaSSIF-V1 and FeSSIF-V2.

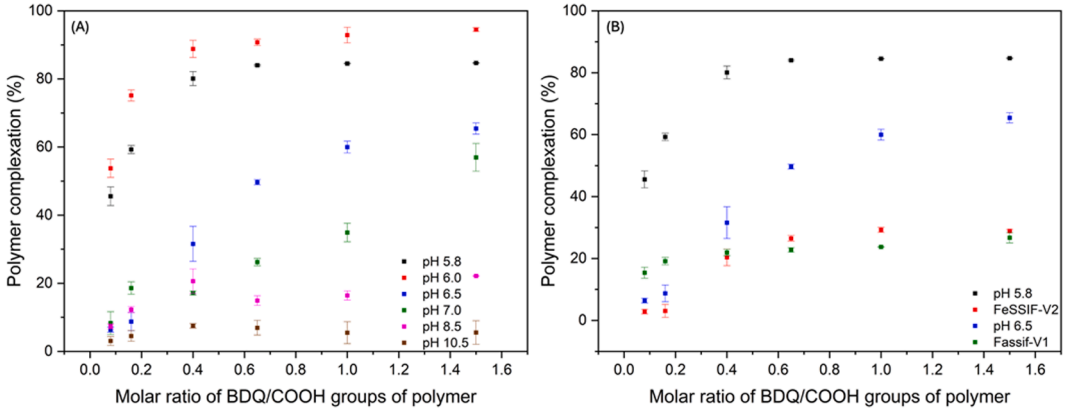


Fig. 2. Percent polymer complexation at different molar ratios of BDQ to COOH groups of HPMCAS MF in (A) buffers pH 5.8, 6.0, 6.5, 7.0, 8.5, 10.5 and (B) buffers pH 5.8, 6.5, FaSSIF-V1 and FeSSIF-V2.

FeSSIF-V2, to a maximum of ~20 % or less for LF and ~30 % or less for MF for all BDQ:COOH ratios tested. Furthermore, the extent of complexation as a function of the molar ratio of BDQ:COOH polymer groups was similar for FaSSIF-V1 and FeSSIF-V2. The composition of the insoluble residue was also estimated, and results are summarized in Table SIV and SV, for BDQ-LF and BDQ-MF, respectively.

ATR-FTIR spectroscopy

ATR-FTIR spectra obtained for the insoluble material formed in BDQ LF and BDQ MF mixtures at different pH conditions are compiled in Fig. 3A and B, respectively. ATR-FTIR spectra of BDQ-LF and BDQ-MF complexes for stock ratios 1 to 5 in pH 5.8, pH 6.0, 6.5, 7.0, 8.5 buffers are compiled in Figure S4 and S5, respectively. The spectra of the

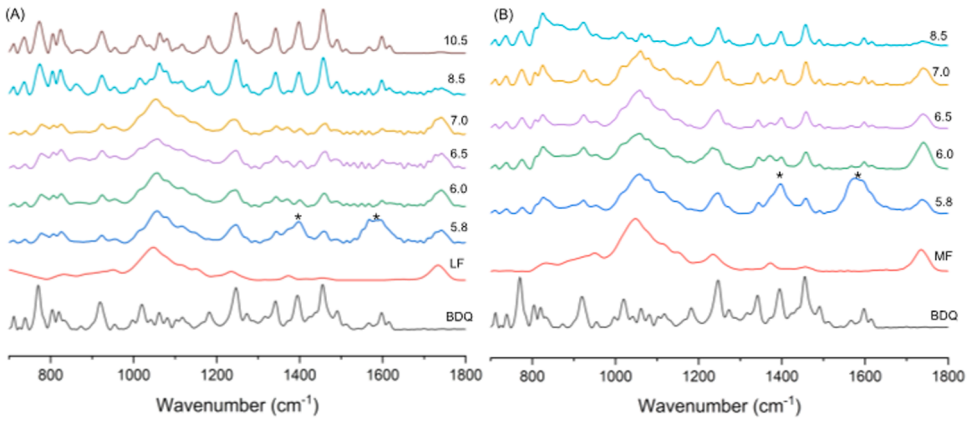


Fig. 3. ATR-FTIR spectra overlays of (A) neat BDQ, neat LF and BDQ-LF complex (R6) obtained after ultracentrifugation from pH 5.8, pH 6.0, 6.5, 7.0, 8.5 and 10.5 buffers. (B) neat BDQ, neat MF and BDQ-MF complex obtained after ultracentrifugation from pH 5.8, pH 6.0, 6.5, 7.0 and 8.5 buffers. Insufficient sample quantity for capturing ATR-FTIR spectra of BDQ-MF complex was obtained for pH 10.5 buffer. The peaks marked with an asterisk for the pH 5.8 sample are assigned to residual citrate salt present in these samples.

insoluble residues were compared with the spectrum of crystalline BDQ, as well as the spectra of neat LF or MF grades of HPMCAS. For samples precipitated at pH values of 6.0, 6.5 or 7.0, a peak was observed at 1720 cm^{-1}, which can be assigned to C=O stretching, indicating the presence of the polymer in the insoluble complex; BDQ does not contain a C=O group. Additional peaks indicated the presence of BDQ in the solid residue, notably in the spectral regions 1210 to 1285 cm^{-1}, 1380 to 1490 cm^{-1} and 1530 to 1650 cm^{-1}, assigned to vibrations of C—N aromatic amine, aromatic C—C and primary N—H groups. These peaks were also seen in the spectrum of crystalline BDQ but are much broader in the complexation samples. This indicates that BDQ is in a disordered form following precipitation in the presence of HPMCAS at these pH values, as would be expected for a drug-polymer ionic complex. In contrast for samples precipitated at pH 8.5 and 10.5, sharper peaks, corresponding to those present in the spectrum of crystalline BDQ are present, indicating substantial crystallization of BDQ. At pH 10.5, peaks characteristic of HPMCAS are essentially absent, consistent with the very low extent of complexation at this pH.

Release profiles of BDQ ASDs

Two-stage release studies were performed by adding ASD powder with either a 5 or 10 % DL to an initial stage of pH 1.6, 3.0, or 5.0 for 60 min followed by a pH 6.5 stage for 60 min, to mimic pH variations resulting from prandial state or comedication with acid reducing agents. Single-stage release studies were also performed at pH 6.5. Results are summarized in Fig. 4.

In the first stage, drug release was poor with <10 % drug released. The highest release was observed in pH 1.6, presumably driven by the higher solubility of the drug at this pH, given that HPMCAS is poorly soluble at low pH. Upon transfer to pH 6.5, additional release was observed, whereby the drug release increased to approximately 20 % for both DLs and both polymer grades. Single stage dissolution at pH 6.5 also led to limited drug release of about 20 % for the 5 % DL ASD, which was reduced when the DL was increased. These observations were similar for ASDs prepared with either grade of HPMCAS. The dissolution vessel was imaged after 120 min, and showed particles settled at the bottom of the vessel (Fig. 5). The residue was examined under polarized light microscope to rule out crystallization of BDQ (Fig. 5). No birefringence was observed, suggesting a lack of crystallization. This was further confirmed using PXRD, where the residue showed a halo pattern, which is typical of a disordered material.

Release studies were also performed in biorelevant media. Release profiles of BDQ-LF and BDQ-MF ASDs in FaSSIF-V1, FeSSIF-V1 and FeSSIF-V2 are summarized in Figs. 6–8, respectively for different DL ASDs. In FaSSIF-V1, 10 % DL BDQ-LF and BDQ-MF ASDs showed 80–90 % release (Fig. 6), with some undissolved material present at 120 min. With an increase in drug loading to 20 %, the extent of release was around 80 % after 120 min.

In FeSSIF-V1, BDQ-LF and BDQ-MF ASDs released to a low extent (20–25 %) due to the low solubility of HPMCAS at pH 5.0 (Fig. 7). In contrast, for FeSSIF-V2 which has a pH of 5.8, both BDQ-LF and BDQ-MF ASDs showed a high extent of release; both 20 and 30 % DL ASDs, showed approximately 90 % release (Fig. 8).

Nucleation induction time

The results of the nucleation induction time measurements of BDQ in the absence and presence of HPMCAS in different media are compiled in Table 3. The nucleation induction time experiment was performed at a

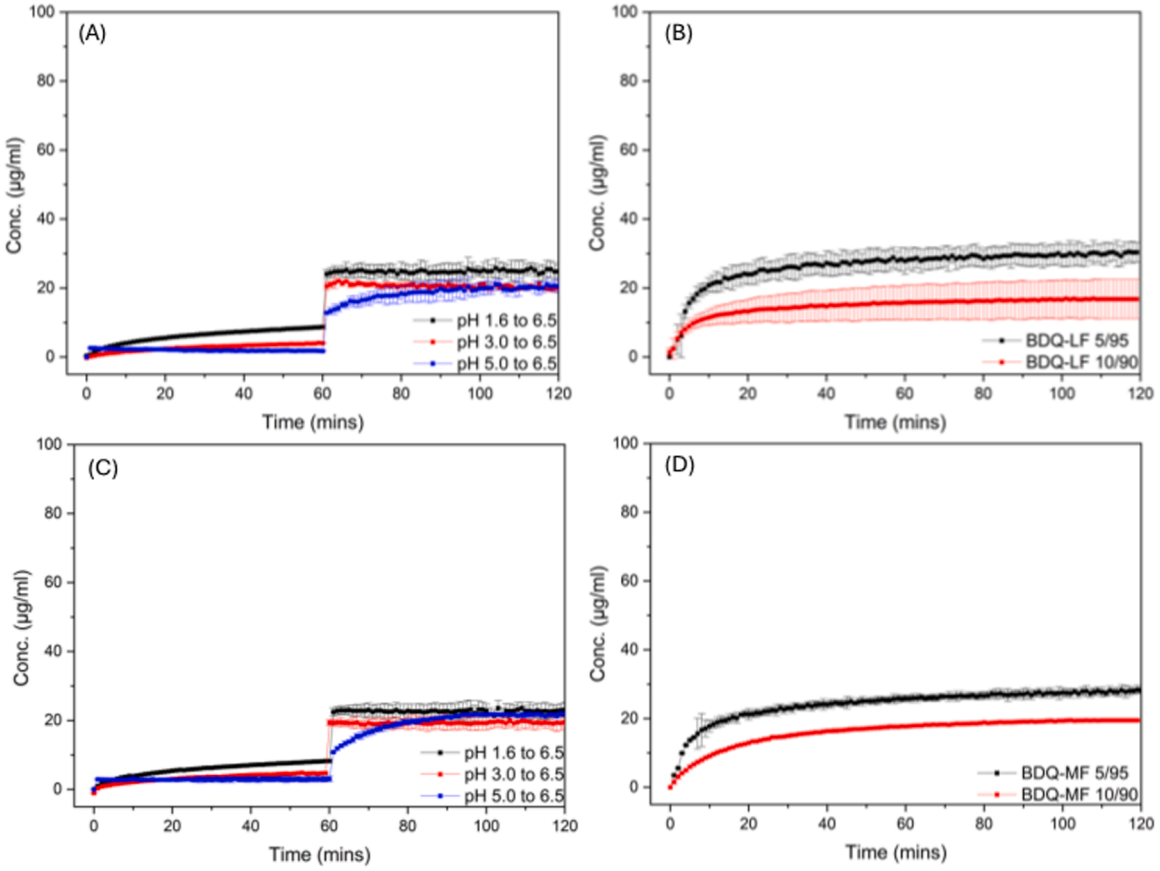


Fig. 4. Release of drug from BDQ-LF 5/95 ASDs in (A) pH switch experiments from an initial stage of 1.6, 3.0, or 5.0 to 6.5 and (B) BDQ-LF 5/95, BDQ-LF 10/90 ASDs in buffer pH 6.5. (C) and (D) depicts release of drug from BDQ-MF 5/95 ASDs in pH switch experiments from an initial stage of 1.6, 3.0, or 5.0 to 6.5 and BDQ-MF 5/95, BDQ-MF 10/90 ASDs in buffer pH 6.5, respectively.

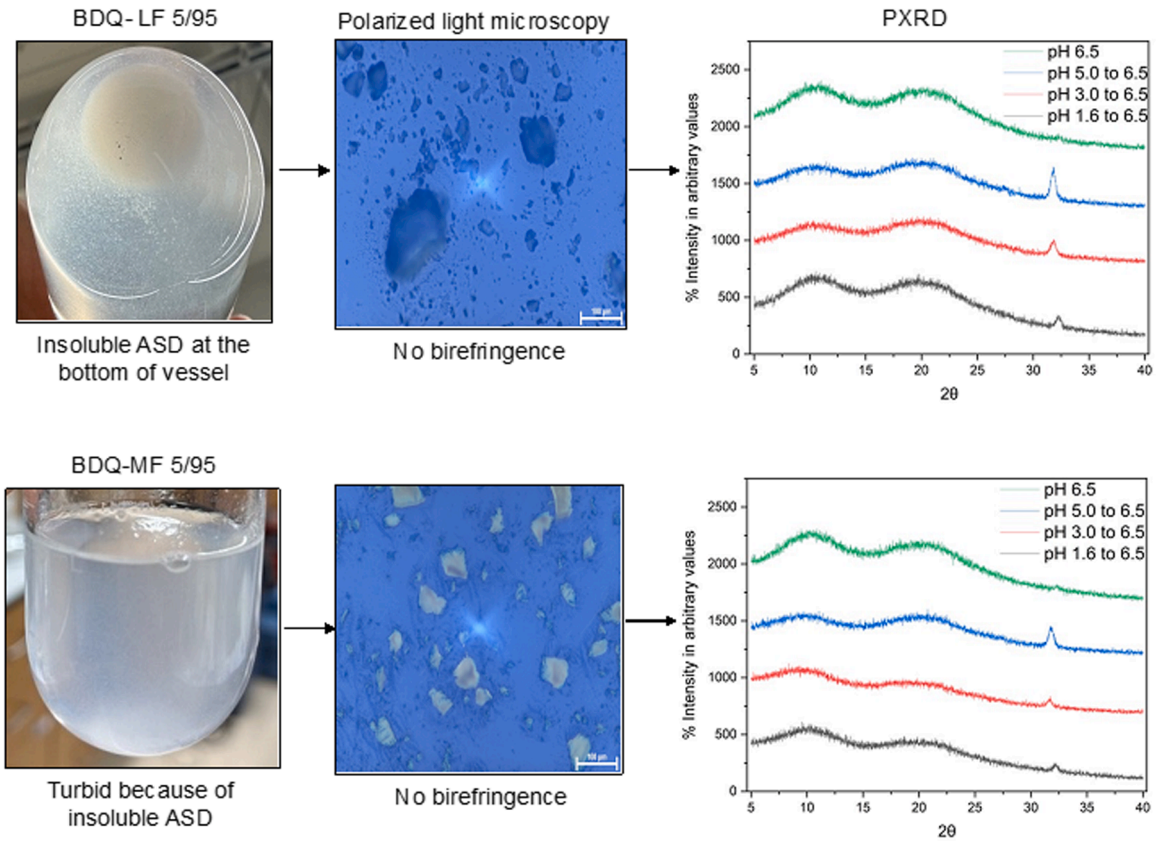


Fig. 5. Representative images of the dissolution vessel at 120 min in buffer pH 6.5 showing turbidity and insoluble ASD at the bottom of the vessel. Polarized light microscope images of the insoluble ASD from buffer pH 6.5 showed no birefringence. PXRD pattern of insoluble ASD collected from each dissolution experiment at 120 min in pH 1.6, 3.0, 5.0 where pH was switched to 6.5 and neat buffer pH 6.5.

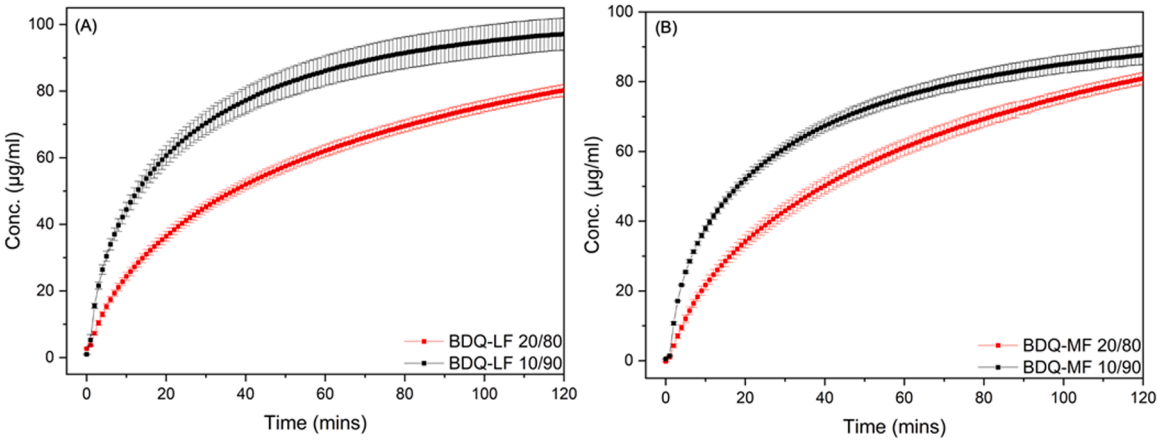


Fig. 6. Release profiles of 10 and 20 % drug loading ASDs (A) BDQ-LF and (B) BDQ-MF in FaSSIF-V1.

BDQ concentration of 100 µg/mL, which is much higher than the amorphous solubility. The amorphous solubility of BDQ at pH 5.8 and 6.5 is only 2 and 0.6 µg/mL, respectively. In the absence of polymer, BDQ precipitated in < 1 min from buffers pH 5.8 and 6.5. The precipitates were greater than 5000 nm, however, they did not show birefringence when evaluated by PLM and remained amorphous for up to 2 h. Birefringence was observed by 3 h. In the presence of polymer (400 µg/mL, equivalent to that generated by dissolution of a 20 % ASD), BDQ again precipitated immediately. However, the precipitates were < 1000 nm in size and remained amorphous for 12–24 h. In FaSSIF-V1 and FeSSIF-V2, no BDQ crystallization was observed for 12–24 h in the presence of the polymer.

XPS

XPS spectra showing the N 1 s peak of various samples are shown in Fig. 9. BDQ free base contained a single N 1 s peak at about 399.5 eV, arising from the two unionized nitrogen atoms in the structure (Figure S1), while the maleate salt had N 1 s peaks at 399 and 402 eV. The latter peak can be assigned to protonated N 1 s, while the former peak is due to the unionized N 1 s peak. It should be noted that BDQ only forms a monoprotic salt, and therefore the maleate salt spectrum should represent the 100 % ionized molecule.[24] The insoluble complex formed by addition of a 1:1 molar ratio of BDQ: COOH groups of HPMCAS MF, as well as the ASD with a 40 % DL, also showed two N 1 s peaks with BEs

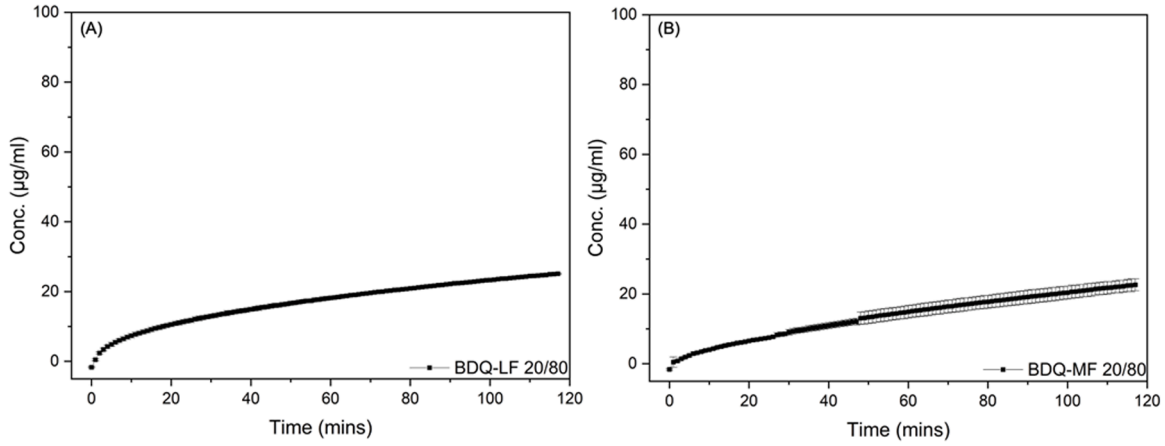


Fig. 7. Release profiles of (A) BDQ-LF 20/80 DL and (B) BDQ-MF 20/80 DL ASDs in FeSSIF-V1.

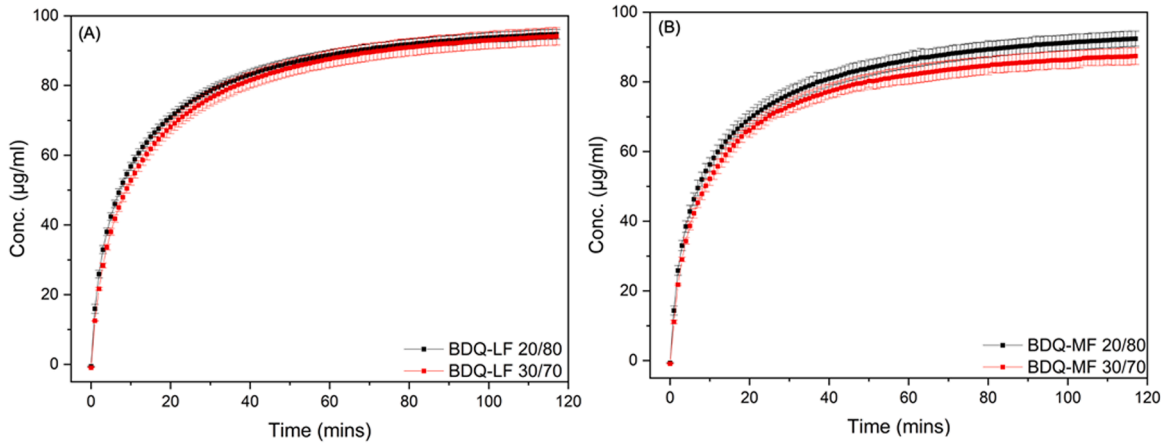


Fig. 8. Release profiles of (A) BDQ-LF 20/80, 30/70 DL and (B) BDQ-MF 20/80, 30/70 DL ASDs in FeSSIF-V2.

Table 3
Nucleation induction time of BDQ (100 µg/mL) in absence and presence of HPMCAS- LF/MF (400 µg/mL) in different media. Size values have been represented as Mean±SD ($N = 3$).

Media	Polymer type and concentration (µg/mL)	Nucleation induction time	Size (nm)
Buffer pH 5.8*	0	No crystallization in 2 h	>7000
	LF; 400	No crystallization in 12 h	604 ± 34
	MF; 400	No crystallization in 21 h	967 ± 30
FeSSIF-V2	0	No crystallization in 12 h	72.7 ± 0.5
	LF; 400	No crystallization in 12 h	98.1 ± 2.5
	MF; 400	No crystallization in 23 h	106.6 ± 1.5
Buffer pH 6.5**	0	No crystallization in 2 h	>6000
	LF; 400	No crystallization in 24 h	650 ± 46
	MF; 400	No crystallization in 23 h	413 ± 16
FaSSIF-V1	0	No crystallization in 12 h	358 ± 28
	LF; 400	No crystallization in 12 h	1002 ± 241
	MF; 400	No crystallization in 24 h	241 ± 35

*Blank FeSSIF-V2 and **Blank FaSSIF-V1. BDQ precipitated in <1 min.

similar to those observe in the maleate salt. The 40 % ASD after suspension in pH 6.5 buffer for 1 h, showed a reduced intensity of the N 1 s at 399 eV. By peak fitting, the percent ionization (with respect to the ionizable N group) was determined for the various samples, with results summarized in Table 4. The controls, BDQ and the BDQ maleate salt showed approximately 0 and 100 % ionization respectively. The insoluble complex and the 40 % DL ASD had similar extents of ionized N, indicating that the formation of ionic interactions between the drug and HPMCAS occurred not only during precipitation, but also during ASD manufacture from organic solvents. The residue harvested following suspension of the 40 % DL in pH 6.5 buffer for 1 h showed a smaller extent of ionized N. From fitting of the C 1 s peak using reference BDQ and HPMCAS-MF spectra, the surface drug concentration was estimated. The 40 % DL ASD showed some polymer enrichment on the surface. The surface concentration of the drug increased after suspension of the ASD in the dissolution medium, indicating preferential loss of polymer from the surface, as has been observed for other systems.[25,26] Notably, approximately 45 % polymer is retained in the sample at the surface post immersion. The insoluble complex formed at a 1:1 molar ratio of BDQ: COOH groups of HPMCAS MF was estimated to contain approximately 52 % drug and 48 % polymer (Table SV). Therefore, the XPS data indicate that polymer is enriched at the surface relative to this estimated bulk composition.

Discussion

HPMCAS is a weakly acidic polymer with a reported pKa of ~5.[9,15,16]

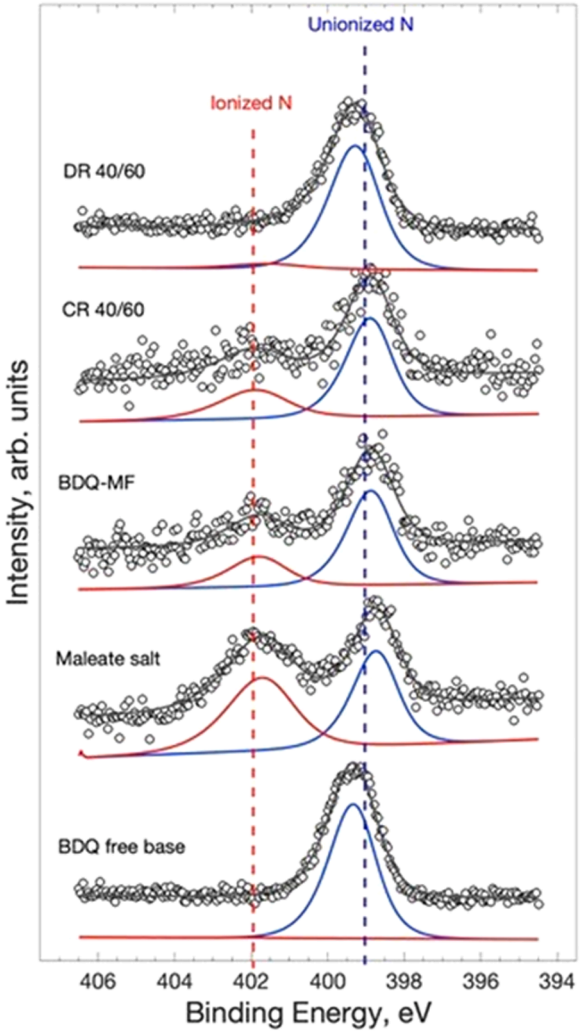


Fig. 9. N 1 s X-ray photoelectron spectra of BDQ in different samples: From bottom to top, BDQ free base, BDQ maleate salt, BDQ-MF 40/60 DL ASD, insoluble residue collected from BDQ-MF complexation experiment (equivalent to R5 sample, Table 1, 1:1 molar ratio BDQ:COOH groups) and BDQ-MF 40/60 DL ASD after immersion in buffer. The spectra are deconvoluted into components corresponding to ionized nitrogen (red) and unionized nitrogen (blue), with vertical dashed lines marking their respective binding energies.

Table 4
XPS-determined percent ionization and surface BDQ concentration from N 1 s and C 1 s analysis, respectively.

Sample	% N protonation *	Surface drug concentration (wt %)
BDQ	4 ± 4	91 ± 8
BDQ maleate salt	101 ± 5	N/A
Insoluble complex	55 ± 4	26 ± 1
40 % DL ASD	52 ± 7	32 ± 2
40 % DL ASD post dissolution	15 ± 3	55 ± 2
HPMCAS	N/A	<1 %

* calculated with respect to the ionizable nitrogen group, rather than the total nitrogen concentration.

It is insoluble at low pH when unionized but is soluble when sufficiently ionized.[27] HPMCAS L and M grades have 1.54 mM and 1.19 mM of COOH groups per gram of polymer, respectively.[16,22] The theoretical percent ionization of HPMCAS as a function of pH, calculated using the Henderson Hasselbalch equation and the reported pKa is shown in Fig. 10. It is apparent that a relatively high extent of ionization, approximately 77 %, is needed for dissolution to commence (this is estimated as from the extent of ionization at the dissolution threshold pH of 5.5).[27,22] Dissolution of HPMCAS at a favorable pH commences with water absorption and ionization at the polymer:solution interface. Ionization leads to additional hydration of polymer chains, swelling and the formation of a thin gel layer, with the concomitant release of H^+ ions which reduce the surface pH to a value lower than the bulk pH. It was reported that the gel layer pH of HPMCAS-MF immersed in pH 6.8 phosphate buffer was reduced to 5.6, 6.0 or 6.2 depending on the buffer capacity (13, 26, or 51 mM/ΔpH, respectively).[14]

The anionic properties of HPMCAS allow for electrostatic interactions with cationic species. Each polymer chain contains multiple COOH groups, hence HPMCAS is classified as a polyelectrolyte. Polyelectrolytes are known to form insoluble complexes with oppositely charged species, including with other polymers, surfactants and small molecules including drugs.[11,28–30] Maximum precipitation typically occurs at the charge neutralization concentration, when electrostatic interactions dominate the formation of the complex.[31] Polyelectrolytes can also interact with other molecules through hydrophobic interactions, whereby the balance of electrostatic and hydrophobic interactions changes as a function of pH.[31,32] The ionization profile of BDQ as a function of pH is shown in Fig. 10. Between pH 5 and 8.5, both BDQ and HPMCAS show some extent of ionization and therefore can potentially form electrostatic interactions. Based on the data shown in Fig. 1A, it is apparent that HPMCAS and BDQ form insoluble complexes, with pH-dependent effects. At pH 10.5, BDQ is mainly unionized, while HPMCAS is predominantly ionized. Therefore, the small extent of insoluble complex formation observed can be attributed to hydrophobic interactions between the drug and polymer. As the pH decreases, BDQ ionization increases, and the extent of insoluble complex formation increased. Maximum mutual ionization occurs at around pH 6.7, where both molecules are about 98 % ionized. Theoretically, the highest extent of complexation is expected at around this pH, however, data collected at pH 6.5 showed a lower extent of complexation than at pH 6.0 or 5.8. This may reflect the high ionization extent of the polymer leading to increased polymer solubility which shifts the equilibrium between dissolved polymer molecules and polymer in the insoluble complex towards the former species. The highest extent of insoluble complexation is observed at pH 5.8 and 6.0. For these pH values, there is a slight excess of BDQ cations relative to HPMCAS carboxylate groups due to a reduction in the ionization extent of HPMCAS as the pH decreases. At pH 6.0 and 5.8, HPMCAS is 91.5 and 88.1 % ionized respectively, while BDQ is >99 % ionized. These values suggest that only a low extent of interaction between the polymer and BDQ is necessary to reduce the number of available ionized groups to below the threshold value of 77 % estimated to be required for polymer solubility (estimated by assuming a

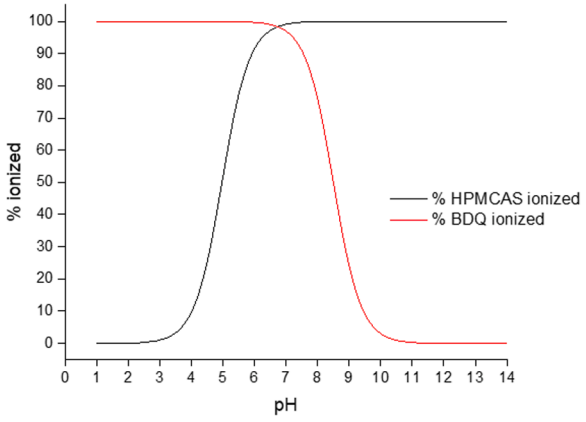


Fig. 10. Theoretical percent ionization of HPMCAS and BDQ as a function of pH.

dissolution pH threshold of 5.5 and a pKa of 5.0). The excess BDQ may explain why complexation is highest at these pH conditions. It should be noted as well that the buffers contained various ionic species, namely the buffer salts as well as NaCl (Table SI). It is well known the electrostatic interactions are impacted by salt concentration due to charge shielding effects.[33,34] Given that BDQ is poorly soluble at pH 5.0 and above (Table 2), it might be expected that the precipitate in the complexation experiments would contain the free base form of the drug. However, XPS analysis (Table 4) confirmed that BDQ was substantially ionized, indicating that drug-polymer ionic interactions were present. Likewise, the ASD also contained evidence of drug-polymer ionic interactions, as observed previously for other ASDs of basic drugs with HPMCAS.[16,35,36]

Importantly, complex formation was considerably reduced in biorelevant media, in both FaSSIF-V1 and FeSSIF-V2. From Table 2, it can be noted that the crystalline solubility is greatly enhanced in both media, indicating a high affinity of the drug for the surfactant micelles present in biorelevant media. Wiedmann and Kamel reviewed the solubilization of multiple drugs by different bile acid micelles and concluded that drug lipophilicity was a key parameter driving solubilization, noting correlations between the mole fraction micelle partition coefficients and octanol-water partition coefficients (log P).[37] BDQ has a log P value of 6.4–7.1 calculated using the online program Chemicalize, (ChemAxon, Budapest, Hungary) and hence can be considered highly lipophilic. However, BDQ is predominantly ionized (Fig. 10) at FaSSIF-V1 and FeSSIF-V2 media pH conditions, whereby ionization has been reported to reduce the extent of solubilization relative to the unionized form.[38] Based on the substantial increases in crystalline solubility, BDQ cations are clearly still able to interact with the mixed micelles present in the simulated intestinal fluids. The positive charge on BDQ may allow for favorable interactions with micelles. This observation is in line with the study from Fagerberg et al., who reported that the solubilization of weakly basic drugs was generally improved in biorelevant dissolution media.[39] The affinity of BDQ molecules for the micelles present in biorelevant media explains the observed reduction in complexation with HPMCAS. In other words, in the presence of both HPMCAS anions and mixed micelles, the tendency of BDQ to form a complex with HPMCAS is reduced by the favorable interactions between BDQ and the micelles.

The release outcomes in different media can be explained by considering the complexation phenomena observed. We start with the premise that drug release is predominantly controlled by polymer dissolution. This is reasonable given that drug release is not improved at low pH, where the drug exhibits much higher solubility. Consistent with a polymer-controlled release mechanism, release extent of the drug from the ASD is low at an acidic pH where the polymer is poorly soluble but increases to some extent when the pH rises to a value where HPMCAS becomes substantially ionized. If the release was drug-controlled, the opposite trend would be expected, given the pH-solubility profile of BDQ (Table 2). The polymer dissolution rate is given by the polymer flux (J_p) across the aqueous boundary layer, which in turn depends on the polymer solubility:

$$J_p = \frac{D_p}{\delta} C_p \quad (1)$$

Where D_p is the polymer diffusion coefficient, C_p is polymer solubility at the polymer-solution interface, and δ is the thickness of the boundary layer. For polymer-controlled release, factors which decrease the polymer solubility will consequently influence drug release. BDQ forms insoluble complexes with HPMCAS for pH conditions where both species are substantially ionized. Furthermore, HPMCAS forms ionic interactions with a portion of the BDQ in the dry ASD, even prior to hydration. The formation, or preexistence of an ionic complex between HPMCAS and BDQ reduces the polymer solubility at the polymer-solution interface and has a catastrophic impact on drug release extent. A second contributing factor is the drug-enrichment observed at the surface of the ASD particle (Table 4). Partial loss of polymer from the particle surface at pH 6.5 is expected based on the extent of polymer complexation observed at this pH (Fig. 2). Given the low solubility of BDQ at this pH (Table 2), surface drug enrichment is expected to be highly unfavorable to release. Hence, when evaluating release in a simple buffer where the second stage pH is 6.5, poor release is observed even when the drug loading is very low, only 5–10 % (Fig. 4). At a 5 and 10 % DL, the molar ratio of BDQ:COOH groups is 0.08:1 and 0.16:1 respectively for HPMCAS-LF. Fig. 1A shows that the extent of insoluble complex formation at these ratios is ~55 and ~75 % at pH 6.0 respectively. The value of pH 6.0 is chosen for the discussion of complexation extent because the gel layer/surface pH is lower than the bulk solution pH, and the reduced solubility of the polymer at the interface will impact its diffusion (Eq. (1)).[14] This highlights that a relatively low extent of complexation between drug and polymer can be extremely detrimental to the release performance. This in turn can be traced back to the critical ionization extent that was estimated for HPMCAS-MF, namely ~77 %. A high extent of ionization is required for polymer solubilization. It is not the ionization *per se*, but rather the hydration resulting from ionization that leads to polymer chain solubilization, although charge repulsion may play a role. Complex formation does not interfere with the ionization process, which is driven by pH, but is expected to impede hydration and hence polymer plasticization, dilution of polymer chains and ultimately release.

At first glance, the observations in simple media would suggest that BDQ is not a good candidate for an ASD formulation with HPMCAS. However, switching the medium to FaSSIF-V1 or FeSSIF-V2 (but not FeSSIF-V1) leads to a dramatic improvement in release, even for higher drug loadings, now suggesting that an ASD with BDQ should have good bioperformance. This is particularly true given the much higher solubility of the amorphous form; based on the data at pH 5.0, the amorphous solubility is >20-fold higher than the crystalline solubility (Table 2). Thus, if the ASD can readily release drug under non-sink conditions, a high supersaturation can be maintained as the drug is absorbed across the biological membrane. The improved release rate in SIFs is partially explained by the disruption of complex formation by the solubilizing components of the SIFs as highlighted in Figs. 6 and 8. Thus, the polymer solubility is higher in the SIFs relative to in the corresponding blank buffers due to reduced complex formation, and this leads to much improved drug release from the ASDs. This is likely the predominant mechanism for the improved release rate in FaSSIF-V1. In FeSSIF-V2, BDQ solubility is very high, and the release studies are no longer conducted under non-sink conditions. Thus, there is a very high driving force for BDQ to release from the ASD into solution. The poor release in FeSSIF-V1 is in line with the supposition of polymer-controlled release given that the polymer is poorly soluble at this pH. The poor polymer solubility in FeSSIF-V1 thus impedes the drug release.

In a previous study from our group, we found that using biorelevant media had no impact on the release profile of delamanid from ASDs with an enteric polymer.[8] Although delamanid is also a weakly basic drug, it has a low pKa, and hence was not extensively ionized at pH conditions where HPMCAS is anionic. A similar outcome was observed when the release rate of neat HPMCAS was compared in blank FaSSIF-V1 or FeSSIF-V2 buffer versus FaSSIF-V1 or FeSSIF-V2, where the polymer release rate was the same in the presence and absence of solubilizing components.[14] Thus, it is likely that the impact of media properties on release from ASDs varies between drugs, and may depend on factors including drug-polymer interaction tendency, as well as the extent of drug solubilization by the medium. Clearly caution should be applied when performing screening studies to identify high performing formulations if simple buffers are used.

Conclusions

Release from bedaquiline-HPMCAS ASDs was found to be highly dependent on dissolution medium pH and composition. Although BDQ is

a weak base and has enhanced solubility at low pH, HPMCAS is insoluble, and release was poor at simulated fasted-state gastric pH conditions. Typically, it would be expected that the drug release would improve when the pH is increased beyond the threshold dissolution pH for the polymer. However, this was not the case and release continued to be low at intestinal pH conditions. The poor release in pH 6.5 buffer was attributed to the formation of an insoluble ionic complex between the drug and polymer, facilitated by a high degree of mutual ionization of drug and polymer at this pH condition. Thus, the oppositely charged species were observed to result in a precipitate, attributed to the formation of hydrophobic ion pairs between the cationic drug and the anionic carboxylate groups of the polymer. Importantly, complex formation was disrupted by the solubilizing species present in simulated intestinal fluids. In turn, release from ASDs was remarkably improved when using biorelevant media, leading to the formation of a highly supersaturated solution of the drug. This additional insight into the occurrence of insoluble complex formation between HPMCAS and a lipophilic cationic drug, as well as the effective disruption of complex formation by micellar species is expected to contribute to improved ASD formulation strategies and in vitro testing approaches.

Supporting information

Chemical structure of BDQ; pKa determination of BDQ; detailed composition of buffers used in the complexation experiment; gradient method for quantification of HPMCAS using HPLC equipped with ELSD; average pH values of the buffers at the end of complexation experiment; solid-state characterization of ASDs- DSC and PXRD; BDQ-LF and BDQ-MF ratios in the insoluble complexation residue. ATR-FTIR spectra overlays of BDQ-LF and BDQ- MF complex obtained in pH 5.8, pH 6.0, 6.5, 7.0, 8.5 and 10.5 buffers.

CRediT authorship contribution statement

Amanpreet Kaur: Methodology, Investigation, Data curation, Writing – original draft, Visualization. **Dmitry Zemlyanov:** Methodology, Investigation, Data curation, Writing – review & editing. **Lynne S. Taylor:** Conceptualization, Writing – review & editing, Supervision, Funding acquisition.

Declaration of competing interest

The authors declare that they have no known competing financial interests or personal relationships that could have appeared to influence the work reported in this paper.

Acknowledgements

The authors would like to acknowledge the Bill and Melinda Gates Foundation (Seattle, WA) for funding this study through award number INV-042627. Under the grant conditions of the Foundation, a Creative Commons Attribution 4.0 Generic License has already been assigned to the Author Accepted Manuscript version that might arise from this submission. AK would like to thank Drs. Van Tu Duong, Dishan Shah and Pradnya Bapat for instrumental support, discussion on complexation, dissolution and amorphous solubility experiments.

Supplementary materials

Supplementary material associated with this article can be found, in the online version, at doi:10.1016/j.xphs.2025.103894.

References

1. Monschke M, Wagner KG. Amorphous solid dispersions of weak bases with pH-dependent soluble polymers to overcome limited bioavailability due to gastric pH variability–an in-vitro approach. *Int J Pharm*. 2019;564:162–170.
2. He Y, Ho C. Amorphous solid dispersions: utilization and challenges in drug discovery and development. *J Pharm Sci*. 2015;104(10):3237–3258.
3. Newman A, Knipp G, Zografi G. Assessing the performance of amorphous solid dispersions. *J Pharm Sci*. 2012;101(4):1355–1377.
4. Newman A, Nagapudi K, Wenslow R. Amorphous solid dispersions: a robust platform to address bioavailability challenges. *Ther Deliv*. 2015;6(2):247–261.
5. Bhujbal SV, Mitra B, Jain U, et al. Pharmaceutical amorphous solid dispersion: a review of manufacturing strategies. *Acta Pharm Sin B*. 2021;11(8):2505–2536.
6. Moseson DE, Tran TB, Karunakaran B, Ambardekar R, Hiew TN. Trends in amorphous solid dispersion drug products approved by the US Food and Drug Administration between 2012 and 2023. *Int J Pharm*. 2024, 100259.
7. Saboo S, Moseson DE, Kestur US, Taylor LS. Patterns of drug release as a function of drug loading from amorphous solid dispersions: a comparison of five different polymers. *Eur J Pharm Sci*. 2020;155, 105514.
8. Van Duong T, Nguyen HT, Taylor LS. Combining enabling formulation strategies to generate supersaturated solutions of delamanid: in situ salt formation during amorphous solid dispersion fabrication for more robust release profiles. *Eur J Pharm Biopharm*. 2022;174:131–143.
9. Butreddy A. Hydroxypropyl methylcellulose acetate succinate as an exceptional polymer for amorphous solid dispersion formulations: a review from bench to clinic. *Eur J Pharm Biopharm*. 2022;177:289–307.
10. Hiew TN, Taylor LS. Combining drug salt formation with amorphous solid dispersions–a double edged sword. *J. Control. Release*. 2022;352:47–60.
11. Bapat P, Paul S, Tseng Y-C, Taylor LS. Interplay of drug–polymer interactions and release performance for HPMCAS-based amorphous solid dispersions. *Mol Pharm*. 2024;21(3):1466–1478.
12. Nguyen HT, Van Duong T, Taylor LS. Enteric coating of tablets containing an amorphous solid dispersion of an enteric polymer and a weakly basic drug: a strategy to enhance in vitro release. *Int J Pharm*. 2023;642, 123139.
13. Nguyen HT, Van Duong T, Taylor LS. Impact of gastric pH variations on the release of amorphous solid dispersion formulations containing a weakly basic drug and enteric polymers. *Mol Pharm*. 2023;20(3):1681–1695.
14. Bapat P, Paul S, Thakral NK, Tseng Y-C, Taylor LS. Does Media choice matter when evaluating the performance of hydroxypropyl methylcellulose acetate succinate-based amorphous solid dispersions? *Mol Pharm*. 2023;20(11):5714–5727.
15. Nguyen DA, Fogler HS. Facilitated diffusion in the dissolution of carboxylic polymers. *AIChE J*. 2005;51(2):415–425.
16. Hiew TN, Zemlyanov DY, Taylor LS. Balancing solid-state stability and dissolution performance of lumefantrine amorphous solid dispersions: the role of polymer choice and drug–polymer interactions. *Mol Pharm*. 2021;19(2):392–413.
17. Mahajan R. Bedaquiline: first FDA-approved tuberculosis drug in 40 years. *Int J Appl Basic Med Res*. 2013;3(1):1–2.
18. US FDA. https://www.accessdata.fda.gov/drugsatfda_docs/label/2024/204384s019lbl.pdf; 2024.
19. Lakshminarayana SB, Huat TB, Ho PC, et al. Comprehensive physicochemical, pharmacokinetic and activity profiling of anti-TB agents. *J Antimicrob Chemother*. 2015;70(3):857–867.
20. Pardhi VP, Patel M, Jain K. Formulation development, characterization, and evaluation of bedaquiline fumarate–Soluplus®–solid dispersion. *Pharm Dev Technol*. 2024:1–12.
21. Taylor LS, Zhang GG. Physical chemistry of supersaturated solutions and implications for oral absorption. *Adv Drug Deliv Rev*. 2016;101:122–142.
22. Bapat P, Taylor LS. Impact of HPMCAS grade on the release of weakly basic drugs from amorphous solid dispersions. *Mol Pharm*. 2024;22(1):397–407.
23. Ilevbare GA, Liu H, Edgar KJ, Taylor LS. Maintaining supersaturation in aqueous drug solutions: impact of different polymers on induction times. *Cryst Growth Des*. 2013;13(2):740–751.
24. Zeller M, Bogdanowich-Knipp S, Smith P, Purcell DK, Okezue M, Smith DT, Byrn SR, Clase KL. Maleate salts of bedaquiline. *Structure Reports*. 2021;77(4):433–445.
25. Dohrn S, Kyeremateng SO, Bochmann E, et al. Thermodynamic modeling of the amorphous solid dispersion-water interfacial layer and its impact on the release mechanism. *Pharmaceutics*. 2023;15(5):1539.
26. Chen Z, Yang K, Huang C, Zhu A, Yu L, Qian F. Surface enrichment and depletion of the active ingredient in spray dried amorphous solid dispersions. *Pharm Res*. 2018;35:1–11.
27. Friesen DT, Shanker R, Crew M, Smithey DT, Curatolo W, Nightingale J. Hydroxypropyl methylcellulose acetate succinate-based spray-dried dispersions: an overview. *Mol Pharm*. 2008;5(6):1003–1019.
28. Sing CE. Development of the modern theory of polymeric complex coacervation. *Adv Colloid Interface Sci*. 2017;239:2–16.
29. Persson B, Hugerth A, Caram-Lelham N, Sundelöf L-O. Dextran sulfate− amphiphile interaction; effect of polyelectrolyte charge density and amphiphile hydrophobicity. *Langmuir*. 2000;16(2):313–317.
30. Goddard E, Hannan R. Cationic polymer/anionic surfactant interactions. *J Colloid Interface Sci*. 1976;55(1):73–79.
31. Khan N, Brettmann B. Intermolecular interactions in polyelectrolyte and surfactant complexes in solution. *Polymers (Basel)*. 2018;11(1):51.
32. Wang H, Wang Y, Yan H, Zhang J, Thomas RK. Binding of sodium dodecyl sulfate with linear and branched polyethyleneimines in aqueous solution at different pH values. *Langmuir*. 2006;22(4):1526–1533.

33. Böckmann RA, Hac A, Heimburg T, Grubmüller H. Effect of sodium chloride on a lipid bilayer. *Biophys J*. 2003;85(3):1647–1655.
34. Xu Q, Hong H, Yu W, Jiang X, Yan X, Wu J. Sodium chloride suppresses the bitterness of protein hydrolysates by decreasing hydrophobic interactions. *J Food Sci*. 2019;84(1):86–91.
35. Song Y, Zemlyanov D, Chen X, et al. Acid-base interactions in amorphous solid dispersions of lumefantrine prepared by spray-drying and hot-melt extrusion using X-ray photoelectron spectroscopy. *Int J Pharm*. 2016;514(2):456–464.
36. Neusaenger AL, Fatina C, Yu J, Yu L. Effect of polymer architecture and acidic group density on the degree of salt formation in amorphous solid dispersions. *Mol Pharm*. 2024;21(7):3375–3382.
37. Wiedmann TS, Kamel L. Examination of the solubilization of drugs by bile salt micelles. *J Pharm Sci*. 2002;91(8):1743–1764.
38. Testa B, Krämer S. *Pharmacokinetic Profiling in Drug Research*. Weinheim, Germany: Wiley-VCH; 2006.
39. Fagerberg JH, Tsinman O, Sun N, Tsinman K, Avdeef A, Bergstrom CA. Dissolution rate and apparent solubility of poorly soluble drugs in biorelevant dissolution media. *Mol Pharm*. 2010;7(5):1419–1430.